 https://doi.org/10.1051/e3sconf/202338501017

Integrated energy operation considering the dependence of multiple wind turbines

Pihua Jiao[1a], Jiajia Chen[1b*], Guoqi Sun[2c], Xu Cai[3d], Lele Wang[1e] and Peibo Sun[1f]

[1]School of Electrical and Electronic Engineering, Shandong University of Technology, Zibo, Shandong, 255000, China
[2]Shandong Deyou Electric Co.,Ltd, Zibo, Shandong, 255000, China
[3]School of Electronic Information and Electrical Engineering, Shanghai Jiao Tong University, Shanghai, 200340, China

Abstract—A key pathway to deep decarbonization of the energy sector is the increased use of wind power in integrated energy systems in the situation of the demand for low-carbon development. However, existing work on wind power in the integrated energy system does not adequately take into account the low carbon emissions in the context of multiple wind turbine dependency. In this respect, it is essential to examine a new type of framework for coordinated operations for meeting operational, low carbon and dependence requirements of multiple wind turbines. Here, a low-carbon oriented electrical-gas-heat energy system including carbon emission, carbon capture and carbon trading is proposed. In particular, the multivariate Gaussian copula in the region is used to investigate the dependence of power output from multiple wind turbines. Results from case studies demonstrate the feasibility of the proposed model in achieving a balanced weigh up between economics and low carbon emissions by the dependence on multiple wind turbines.

1. Introduction

In recent years, global warming and pollution have become increasingly important issues. For the sustainability of human society, it is important to promote the reduction of carbon dioxide for moving to a low-carbon economy [1]. With this in mind, the technology of integrated energy systems (IES), consisting of wind power, gas-fired generation and combined heat and power (CHP), has attracted more attention in recent years, due to its high efficiency in generating electricity and low carbon intensity [2]. Complementarity between different energy sources is the key feature of the IES, but it does not effectively address the problem of carbon dioxide emissions. Research into an effective low-carbon IES operating framework is therefore urgently needed in the era of low-carbon development around the world.

Additionally, in the energy system with large centralized wind turbine integration, the performance of different wind turbines is generally considered to be independent [3]. Indeed, the spatial dependency and coupling of wind power cannot be ignored. Failure to do so will have the effect of operation due to inaccurate power flow calculations. In [4], Linear regression and the Cholesky decomposition are each developed to describe the correlation between the two. However, the above techniques are based on the assumption that the relationship is linear with constant matrices. The non-linear revelation approach based on the Nataf transformation, a kind of copula technique, is proposed to address this problem [5]. It is an approach that is revelatory. It is possible to arrive at a recognized practice in a short space of time schedule by assuming that the errors will follow the Gaussian distribution [6]. Moreover, a sufficiently large non-Gaussian variable follows an almost Gaussian distribution, which is based on the central limit theorem [7]. In fact, obtaining the joint distribution is the simplest way to fully describe the correlations of random variables. To represent the joint distribution of wind speeds associated with different wind turbines and capture dependencies between different wind turbines, the multivariate Weibull function is derived, but the assumed distribution may not correspond to reality [8]. A powerful tool for fitting the joint distribution of wind power is the Gaussian Mixture Model. However, it is difficult to implement a multivariate parameter estimation when the dimension of the random inputs is very large. Therefore, to obtain the power correlation between multiple wind turbines, an advanced parametric estimation method, multivariate Gaussian copula, is proposed.

Low carbon emissions under the dependence on multiple wind turbines, however, are not adequately considered in existing work on integrated IES, which is reflected in a lack of economic efficiency in the planning decisions. Therefore, the low-carbon oriented integrated energy operation considering the dependence of multiple wind turbines is proposed to study the couplings of outputs of multiple wind turbines, which targets determining the dependent structure among multiple wind turbines in IES, so as to decouple the dependence of regional wind turbines.

[a]jiaopihua2013@163.com, [b*]20604010003@sdut.edu.cn, [c]sunguoqi09@163.com, [d]scaixu412@163.com, [e]wanglelepj@163.com, [f]sungpeibott@163.com

2. Integrated energy system description and mathematical modelling

The main objective aims to achieve the coordinated operation for a low-carbon oriented integrated electricity-gas-heat energy system, which is established on the basis of multiple energy sectors including natural gas-fired generators, coal-fired generators, and CHP units, electric boilers (EB) and wind turbines.

2.1. Objective

In order to realize the economic operation of the low-carbon oriented IES, the objective of the proposed IES framework for coordination operation is to minimize the total operation cost. The objective function is presented as follows:

$$OC = f_{\mathrm{CCS}} + f_{\mathrm{CT}} + f_{\mathrm{GC}} + f_{\mathrm{GW}} + f_{\mathrm{CHP}} \quad (1)$$

$$f_{\mathrm{CCS}} = \sum_{t=1}^{T} \eta Q_t^{\mathrm{CEV}} \quad (2)$$

$$f_{\mathrm{CT}} = \sum_{t=1}^{T} \chi_{\mathrm{CT}} \left(Q_t^{\mathrm{CEV,C}} - Q_t^{\mathrm{CQ}} + Q_t^{\mathrm{CEV,G}} - Q_t^{\mathrm{CG}} \right) \quad (3)$$

$$f_{\mathrm{GC}} = \sum_{t=1}^{T} \left[\sum_{i=1}^{N_{\mathrm{GS}}} \left(a_i^{\mathrm{GS}} + b_i^{\mathrm{GS}} P_{i,\mathrm{t}}^{\mathrm{GS}} + c_i^{\mathrm{GS}} P_{i,\mathrm{t}}^{\mathrm{GS2}} \right) \right] \quad (4)$$

$$f_{\mathrm{GW}} = \sum_{t=1}^{T} \left[\chi_{\mathrm{GW}} \left(\sum_{i=1}^{N_{\mathrm{GW}}} G_{i,t}^{\mathrm{GW}} \right) \right] \quad (5)$$

$$f_{\mathrm{CHP}} = \sum_{t=1}^{T} \left[\sum_{i=1}^{N_{\mathrm{CHP}}} \chi_{\mathrm{CHP}} \left(\gamma_{\mathrm{P}} P_{i,t}^{\mathrm{CHP}} + \gamma_{\mathrm{H}} H_{i,t}^{\mathrm{CHP}} \right) \right] \quad (6)$$

where $Q_t^{\mathrm{CEV}} = Q_t^{\mathrm{CEV,C}} + Q_t^{\mathrm{CEV,G}}$, $Q_t^{\mathrm{CEV,C}}$ and $Q_t^{\mathrm{CEV,G}}$ represent the carbon emission volume of coal-fired and gas-fired generation at time t, respectively, Q_t^{CQ} and Q_t^{GQ} are the allocated carbon quota of coal-fired generation and gas-fired generation at time t, respectively. Equation (11) denotes the generation cost of units, where $P_{i,\mathrm{t}}^{\mathrm{GS}}$ is the power output of the ith unit at time t, a_i^{GS}, b_i^{GS} and c_i^{GS} represent the cost coefficients corresponding to the ith unit, N_{GS} denotes the number of coal-fired and gas-fired generators. In Equation (4), f_{GW} represents the gas production cost from gas wells, where N_{GW} is the number of gas wells, $G_{i,t}^{\mathrm{GW}}$ denotes the gas production of gas well i at time t, χ_{GW} is the gas price. Equation (5) expresses the operation cost of CHP generators, where N_{CHP} represents the number of CHP generators, $H_{i,t}^{\mathrm{CHP}}$ and $P_{i,t}^{\mathrm{CHP}}$ are the heat power and electrical power generated by the CHP generator i at time t, respectively, χ_{CHP} is the cost coefficient of CHP generators, γ_{P} and γ_{H} represent the coefficients to describe the relationship between the fuel consumed by the electric power and the thermal power of the CHP generator, respectively.

2.2. Electricity network constraints

The power flow $PF_{l,t}$ in line l is:

$$PF_{l,t} = \left(\theta_{v,t} - \theta_{\mathrm{w},t} \right) / Im_l \quad (7)$$

where $\theta_{v,t}$ and $\theta_{\mathrm{w},t}$ denote respectively the voltage angle of nodes v and w in line l at time t, and Im_l represents the impedance of line l.

The operation constraints of generation including output constraint, ramping up and ramping down constraints, are formulated as:

$$P_{i,\min}^{\mathrm{GS}} \le P_{i,\mathrm{t}}^{\mathrm{GS}} \le P_{i,\max}^{\mathrm{GS}} \quad (8)$$

$$P_{i,t}^{\mathrm{GS}} - P_{i,t-1}^{\mathrm{GS}} \le R_{\mathrm{U},i} \quad (9)$$

$$P_{i,t+1}^{\mathrm{GS}} - P_{i,t}^{\mathrm{GS}} \le R_{\mathrm{D},i} \quad (10)$$

where $P_{i,\min}^{\mathrm{GS}}$ and $P_{i,\max}^{\mathrm{GS}}$ are respectively the lower and upper limits of power output $P_i^{\mathrm{GS}} \in \left\{ P_i^{\mathrm{C}}, P_i^{\mathrm{W}}, P_i^{\mathrm{G}}, P_i^{\mathrm{CHP}}, P_i^{\mathrm{EB}} \right\}$, $R_{\mathrm{U},i}$ and $R_{\mathrm{D},i}$ are the limits of ramping up and ramping down of the ith unit, respectively.

The power balance constraint is shown as:

$$P_t^{\mathrm{C}} + P_t^{\mathrm{G}} + P_t^{\mathrm{W}} + P_t^{\mathrm{CHP}} + PF_t - P_t^{\mathrm{D}} - P_t^{\mathrm{EB}} = 0 \quad (11)$$

where P_t^{D}, P_t^{W} and P_t^{CHP} are the load demand, power output of wind turbine and CHP generator at time t, respectively.

2.3. Natural gas network constraints

In this paper, the model of the main components of the proposed natural gas network involves gas well, gas pipeline, compressor and gas load.

The gas productions of the gas well $G_{i,t}^{\mathrm{GW}}$ and nodal pressure $p_{k,t}$ are limited:

$$G_{i,\min}^{\mathrm{GW}} \le G_{i,t}^{\mathrm{GW}} \le G_{i,\max}^{\mathrm{GW}} \quad (12)$$

$$p_k^{\min} \le p_{k,t} \le p_k^{\max} \quad (13)$$

where $G_{i,\min}^{\mathrm{GW}}$ and $G_{i,\max}^{\mathrm{GW}}$ are the lower and upper limits for gas production of gas well i, respectively, $p_k^{\min}$ and $p_k^{\max}$ denote the minimum and maximum of the kth nodal pressure, respectively.

Then, the gas flow model can be expressed as:

$$G_{k,n,t}^{\mathrm{GF}} = c_{k,n} \sqrt{\left| p_{k,t}^2 - p_{\mathrm{n},t}^2 \right|} \quad (14)$$

where $G_{k,n,t}^{\mathrm{GF}}$ is the gas flow from node k to node n at time t, and $c_{k,n}$ is a parameter related to the pipeline.

Moreover, the relationship between outlet pressure $P_{j,t}$ through the compressor and inlet pressure $P_{n,t}$ can be expressed as $P_{j,t}=\rho_t \times P_{n,t}$, where ρ_t is the compression ratio of compressor.

The gas balance equation in the natural gas network is expressed as:

$$G_t^{\mathrm{GW}} + G_t^{\mathrm{GF}} - G_t^{\mathrm{GAS}} - G_t^{\mathrm{G}} - G_t^{\mathrm{CHP}} = 0 \tag{15}$$

where G_t^{GAS}, G_t^{G} and G_t^{CHP} are respectively the natural gas load demand, the consumption of gas-fired generators and CHP generators at time *t*.

2.4. Heating network constraints

The heat sources incorporate CHP generator and electric boiler. The relationship between heat production H_t^{EB} and electricity consumption P_t^{EB} of electric boiler at time *t* is expressed in Equation (16). Similarly, the relationship between heat production H_t^{CHP} and electricity consumption P_t^{CHP} of CHP at time *t* is shown in Equation (17).

$$H_t^{\mathrm{EB}} = \varepsilon^{\mathrm{EB}} P_t^{\mathrm{EB}} \tag{16}$$

$$H_t^{\mathrm{CHP}} = \varepsilon^{\mathrm{CHP}} P_t^{\mathrm{CHP}} \tag{17}$$

where $\varepsilon^{\mathrm{EB}}$ and $\varepsilon^{\mathrm{CHP}}$ are the power-heat conversion efficiency of EB and CHP, respectively.

In the condition of mass flow rates, the nodal temperatures are formulated as:

$$T_{\mathrm{ms,in}} ms_{\mathrm{in}} = T_{\mathrm{ms,out}} ms_{\mathrm{out}} \tag{18}$$

$$T_{\mathrm{mr,in}} mr_{\mathrm{in}} = T_{\mathrm{mr,out}} mr_{\mathrm{out}} \tag{19}$$

where $T_{\mathrm{ms,in}}$, $T_{\mathrm{ms,out}}$, $T_{\mathrm{mr,in}}$ and $T_{\mathrm{mr,out}}$ are respectively the nodal temperature before and after the water mixes in the supply and return pipes, ms_{in}, ms_{out}, mr_{in} and mr_{out} denote the mass flow rates before and after the water mixes in the supply and return pipes, respectively. The water outflowing temperature equals to the mixed temperature, i.e., $T_{\mathrm{ms,out}}=T_{\mathrm{ms}}$, $T_{\mathrm{mr,out}}=T_{\mathrm{mr}}$, T_{ms} and T_{mr} are the mixing nodal temperature of the water supply pipes and the return pipes, respectively.

The relationship between the heat load and temperature can be expressed as:

$$H_t^D = C_{\mathrm{p}} m_t \left(T_{\mathrm{ms}} - T_{\mathrm{mr}}\right) \tag{20}$$

where H_t^D is the heat load at time *t*, C_{p} is the heat capacity of water, and m_t is the amount of water injected at time *t*.

The heat load balance of heating network is

$$H_t^D - H_t^{\mathrm{CHP}} - H_t^{\mathrm{EB}} = 0 \tag{21}$$

3. The dependence of multiple wind turbines

Wind turbines always gather in the region with rich wind resources. Hence, the dependence of regional wind power for multiple wind turbines should be considered under the circumstance of large-scale wind energy integration. In this paper, we propose a multivariate Gaussian copula function for the sake of obtaining the correlation among multiple wind turbines and sampling procedure of wind power.

With regard to a vector $w = [w_1,\ldots,w_d]$ of wind power outputs from *d* wind turbines, the joint distribution function *M* can be obtained by the connection of marginal distribution functions with the unique copula function *C*.

$$M\left(w_1,..,w_d\right) = C\left(F\left(w_1\right),\mathrm{L}\ ,F\left(w_d\right)\right) \tag{22}$$

$$C\left(u_1,\mathrm{L}\ ,u_d\right) = M\left(F^{-1}\left(u_1\right),\mathrm{L}\ ,F^{-1}\left(u_d\right)\right) \tag{23}$$

where $u_i = F(w_i)$, $F(w_i)$ is the cumulative distribution function (CDF) of w_i for *i*th wind turbine.

Then, the probability density function (PDF) *m* of *M* can be obtained by

$$m\left(w_1,w_2,\cdots,w_d\right) = \frac{\partial^d C\left(u_1,\cdots,u_d\right)}{\partial u_1 \cdots \partial u_d} \frac{\partial F\left(w_1\right)}{\partial w_1} \cdots \frac{\partial F\left(w_d\right)}{\partial w_d} \tag{24}$$

The multivariate Gaussian copula function of *d* different wind turbines is given by

$$M\left(w_1,w_2,\cdots,w_d\right) = \int_0^{u_1} \cdots \int_0^{u_d} \frac{1}{\left(2\pi\right)^{d/2} \left|A\right|^{1/2}} \exp\left\{-\frac{1}{2}\left(u_1,\cdots,u_d\right)^{\mathrm{T}} A^{-1}\left(\left(u_1,\cdots,u_d\right)\right)\right\} du_1 \cdots du_d \tag{25}$$

where *A* is the covariance matrix of wind power outputs from different wind turbines.

The Sobol sequence is introduced to study the sampling of wind power for different wind turbines.

4. Case study

We make a comparison for the IES with and without dependence of multiple wind turbines of wind power from different wind turbines, which is shown in Fig. 1. The case without the dependence of multiple wind turbines is involved in "Case 2" and the case considering the dependence of multiple wind turbines is set in "Case 2".

Table 1. Dispatching results with and without considering the dependence of multiple wind turbines.

Parameters	Case 1	Case 2
Total cost (10^6\$)	4.0361	3.8009
Low-carbon emission cost (10^5\$)	2.5946	0.8177
Total coal-fired generation (MWh)	159.8796	142.4909
Total gas-fired generation (MWh)	275.3335	284.3448
Total wind power generation (MWh)	644.5865	661.9752
Total CHP generation (MWh)	36.8522	42.5228

https://doi.org/10.1051/e3sconf/202338501017

Total electric boiler (MWh)	12.9393	7.2687

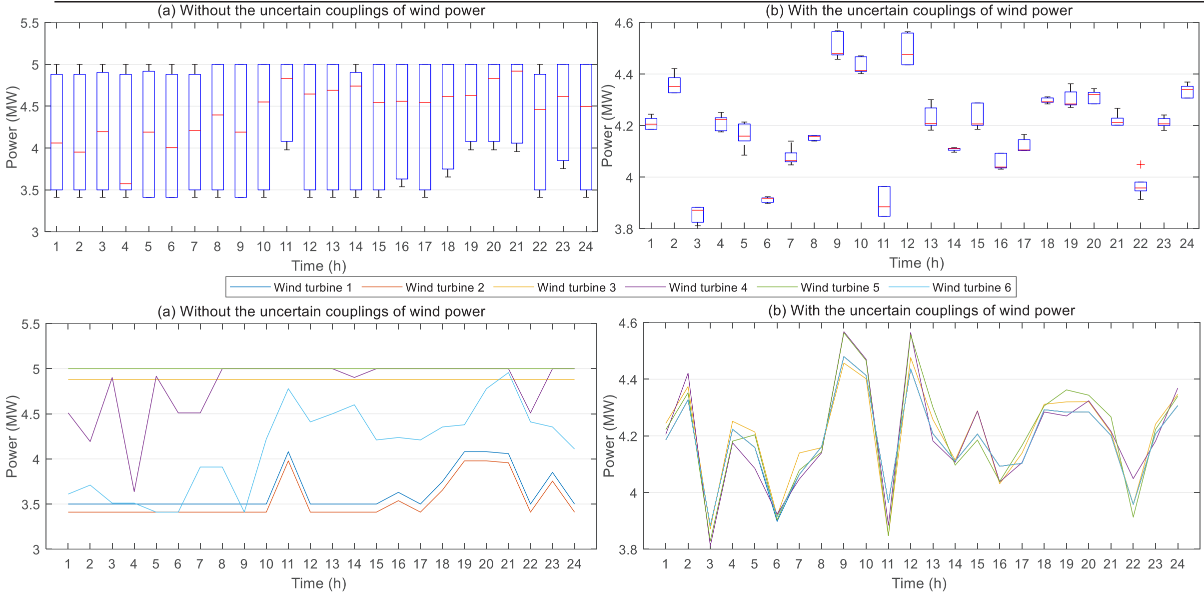

Fig.1 IES operation with and without the dependence of multiple wind turbines

Combining Fig. 1 and Table 1, it can be observed in Case 2 that the power curves of wind turbines are more compact in the situation of considering the uncertain couplings, and the power curves of wind turbines in Case 1 are loosely distributed nevertheless. Furthermore, the power output of wind turbines in Case 2 improves 17.3887 MWh and the operation cost reduces 0.2352×10^6\$ comparing to that of Case 1. Therefore, Case 2 considering the uncertain couplings promotes the correlation of multiple wind turbines, has the advantages of compact distribution, and reduces the uncertain risk of integrated wind power on the basis of ensuring operation costs. Furthermore, the Spearman correlation coefficient ρ_s and the Kendal correlation coefficient ρ_k are employed to describe the linear correlation and consistent correlation between the marginal distributions. By the calculation, ρ_s and ρ_k in Case 2 are respectively 0.8696 and 0.9637, larger than 0.7841 and 0.8945 of Case 1, and the probability of the same variation trend in Case 2 is higher than that of Case 1. Therefore, the IES operation considering the uncertain couplings of wind turbines can better reflect the mutual relationship between wind turbines, thereby reducing the error caused by the correlation of wind turbines output.

5. Conclusion

In this paper, a novel model for integrated energy system considering carbon emission and dependence of multiple wind turbines is proposed consisting of electricity, gas and heating systems with the dependence of multiple wind turbines. This paper aims to meet and balance the operation economy, dependence requirements, wind power accommodation, carbon emission reduction effectively and efficiently by controlling the level of carbon intensity. Case studies demonstrate that the coordinated operation of the integrated electricity-gas-heat energy system considering the carbon emission can reduce the system operation costs and carbon emission to some extent. Detailedly, the IES operation cost with the dependence of multiple wind turbines reduces 0.2352×10^6\$, and the operation cost reduces 5.83% compared to those without the dependence of multiple wind turbines. Furthermore, it is necessary to consider the correlation of uncertain wind power, and multivariate Gaussian Copula is effective in describing the dependence and complicated correlation among random variables of wind power among different wind turbines.

Acknowledgments

This work was supported by the Project of Shandong Provincial Key Program (2019JZZY020804).

References

1. Lin B, Li Z. (2022) Towards world's low carbon development: The role of clean energy. Applied Energy, 307:1–9.
2. käheimo J, Weiss R, Kiviluoma J, Pursiheimo E, Lindroos TJ. (2022) Impact of power-to-gas on the cost and design of the future low-carbon urban energy system. Applied Energy, 305:1–20.
3. Guo Y, Ming B, Huang Q, Liu P, Wang Y, Fang W, et al. (2022) Evaluating effects of battery storage on day-ahead generation scheduling of large hydro wind photovoltaic complementary systems. Applied Energy, 324:1–21
4. Xu X, Yan Z. (2017) Probabilistic load flow calculation with quasi-monte carlo and multiple linear regression. International Journal of Electrical Power & Energy Systems, 88:1–12.
5. Xiao Q. (2015) Comparing three methods for solving probabilistic optimal power flow. Electric Power Systems Research, 124:92–99.
6. Jiao P, Chen J, Cai X, Wang L, Zhao Y, Zhang X. (2021) Joint active and reactive for allocation of renewable energy and energy storage under

https://doi.org/10.1051/e3sconf/202338501017

uncertain coupling. Applied Energy, 302:1–19.
7. Mandelbrot BB. (1997) The variation of certain speculative prices, 7:371–418.
8. Villanueva D, Feijóo A, Pazos JL. (2013) Multivariate weibull distribution for wind speed and wind power behavior assessment. Resources, 2:370–384.